

Dynamic indentation on human skin *in vivo*: ageing effects

G. Boyer^{1,2}, L. Laquière¹, A. Le Bot¹, S. Laquière² and H. Zahouani¹

¹Laboratory of Tribology and System Dynamics, UMR CNRS 5513, ENISE-ECL, Ecully, France and ²Laboratory PERITESCO, Paris, France

Background/purpose: Knowledge of the mechanical properties of the human skin is very important for cosmetic and clinical research. Objective and quantitative measurements are essential to compare studies performed by different experimenters in different centres. The aim of this paper is to present a method to measure the viscoelastic properties of human skin *in vivo* using dynamic indentation.

Methods: A complete device to assess the stiffness and damping of skin has been developed. The frequency and strain amplitude range from 10 to 60 Hz and from 1 to 10 μm . Tests on pure elastic inert materials have been performed to validate the device. An *in vivo* study including dynamic indentation, suction test, hydration measurement and topographic analysis has been performed on 46 subjects aged from 18 to 70 years, divided into three groups.

Results: Results on inert materials show the validity of the device developed. The mechanical behaviour of the skin can be described by a Kelvin–Voigt model under dynamic

indentation. A comparison with a suction test, hydration and topographic measurements shows that the stiffness and the damping measured by dynamic indentation correspond mainly to the natural tense state of the skin on the body due to the dermis. A weak correlation has been found between dynamic indentation and suction parameters. The complex modulus measured by dynamic indentation at 10 Hz frequency stress ranges from 7.2 ± 2.1 kPa for the oldest group to 10.7 ± 2.6 kPa for the youngest group.

Conclusion: The device presented gives convincing results. The measurement of stiffness and damping complements the viscoelastic phenomenological parameters of the suction test.

Key words: dynamic indentation – stiffness – damping – viscoelasticity – topography

© Blackwell Munksgaard, 2008

Accepted for publication 28 December 2007

HUMAN SKIN is the heaviest and the vastest organ of the human body. As it is the interface between the external environment and the body, its function is vital. Its three-layer composition imparts very particular mechanical properties to the skin. It is a heterogeneous, anisotropic, adhesive material showing a non-linear stress–strain relationship. Its mechanical behaviour is also very complex (1). Knowledge of these properties is essential for cosmetic and clinical research. The touch of dermatologists or cosmetologists is often used to assess skin properties. However, objective and quantitative measurements are essential to compare studies performed by different experimenters in different centres. Many devices with various techniques have been used to measure the mechanical properties of the skin *in vivo*, such as indentation (2, 3), suction (4–6), torsion (7, 8), wave propagation (9), extensometer (10, 11) and ballistometer (12) techniques. Measurement of dynamic properties is also very interesting. Dynamic studies using a torsion device (13) or

tangential stress (14) have already been carried out. Although dynamic mechanical analysis (15) using indentation is often used on polymer materials (16, 17), no application on human skin has been realized. The aim of this paper is to propose an application of dynamic indentation on human skin *in vivo* using a specially developed device. As the mechanical properties of the skin are mainly due to the epidermis and the dermis, which are very thin, a strain amplitude of a few microns has been chosen to minimize the underlying structure effects. Tests on pure elastic materials with various stiffnesses have been performed to validate the device. An *in vivo* study on 46 subjects aged from 18 to 70 years has been carried out. Dynamic indentation, suction test and epidermal hydration measurement have been carried out. Skin replicas of the studied area were obtained to look for any correlation between skin microrelief, stiffness and elasticity measurements. The body mass index (BMI) was calculated to study the hypodermis influence.

Materials and Methods

Dynamic indentation material

Theory

Although it is composed of three layers with different mechanical properties, the skin reacts like a monolayer material. This justifies, as a first approximation, studying the whole mechanical behaviour of the skin as if it were a homogeneous material (1). In our case, a sine displacement $u(t)$ (m) is applied to the skin surface with an indenter. The resulting force $F(t)$ is measured. As a viscoelastic material, the indenter/skin contact can also be represented by Fig. 1.

m (kg) is the mass of the indenter. $F(t)$ (N) is a sine force of angular frequency ω (rad/s) and amplitude f_0 (N), given by

$$F(t) = f_0 \sin(\omega t). \quad (1)$$

The spring with stiffness $K(\omega)$ (N/m) represents the elastic part, and the dash pot with damping $C(\omega)$ (Ns/m) represents the viscous part. The behaviour of the indenter/skin contact system is described by the linear differential equation

$$m\ddot{u}(t) + C(\omega)\dot{u}(t) + K(\omega)u(t) = f_0 \sin(\omega t). \quad (2)$$

The displacement $u(t)$ has the same angular frequency as the force, but with a phasingout φ (rad) given by

$$u(t) = u_0 \sin(\omega t - \varphi) \quad (3)$$

where u_0 (m) is the displacement amplitude. The phasingout is given by

$$\varphi = \arctg\left(\frac{2\xi\beta}{1 - \beta^2}\right) \quad (4)$$

with

$$\omega_0 = \sqrt{K(\omega)/m} \quad (5)$$

$$\beta = \frac{\omega}{\omega_0} \quad (6)$$

$$\xi = \frac{C(\omega)}{2m\omega_0} \quad (7)$$

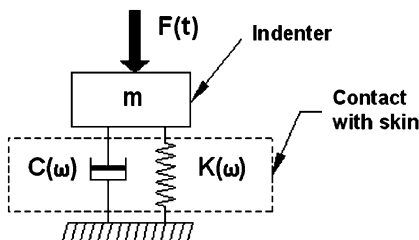


Fig. 1. Indenter/skin contact model.

where ω_0 (rad/s) is the natural angular frequency of the indenter/skin contact system, β is the ratio of the force angular frequency and the natural angular frequency and ξ (MPa/kg/rad) is the modal damping factor.

With Eq. (5), the natural angular frequency of the indenter/skin contact system appears. Below this frequency, the phasingout is lower than 90° . The contact force is dominant. Above this frequency, the phasingout is greater than 90° . The inertia force of the indenter is dominant.

The stiffness and the damping are given by the following equations (18):

$$K(\omega) = \left| \frac{f_0}{u_0} \right| \cos(\varphi) + m\omega^2 \quad (8)$$

$$C(\omega) = \left| \frac{f_0}{u_0} \right| \frac{\sin(\varphi)}{\omega} \quad (9)$$

The simultaneous measurement of the force and displacement is sufficient to determine the viscoelastic properties $K(\omega)$ and $C(\omega)$ of the indenter/skin contact.

In the first instance, the skin is considered to be semi-infinite body with linear behaviour, indented by an axisymmetric indenter of radius a (m). The complex modulus E^* (MPa), with a real part E'^* (MPa) corresponding to the elastic behaviour and an imaginary part E''^* (MPa) corresponding to the viscous behaviour, is given by (19)

$$E^* = E'^* + iE''^* \quad (10)$$

$$E'^* = \frac{K(\omega)}{2a} \quad (11)$$

$$E''^* = \frac{C(\omega)\omega}{2a} \quad (12)$$

Material

The force and displacement of the indenter on the skin are measured by an impedance head (Brüel & Kjaer, Nærum, Denmark). This head consists of a very rigid body made of titanium, with an accelerometer and a force sensor inside. Both sensors are of piezoelectric material. They only record dynamic signals. The main advantage of using this impedance head is the coaxiality between the accelerometer and the force sensor, which minimizes the disturbance phasingout.

The indenter is cylindrical with a radius of 2 mm. This shape minimizes the adhesive effect of the skin (20), because the contact radius is constant with the indenter penetration. The in-

denter is screwed on the force sensor. The total mass on the force sensor is 4.2 g.

In order to reach a very small amplitude, a piezoelectric translation stage has been used in our application (Piezosystem jena, Hopedale, MA, USA). A constant amplitude of motion from 1 to 10 μm for a frequency ranging from 10 to 60 Hz is obtained. It is important to maintain a constant amplitude displacement during the frequency scan to stress the same area. As the translation stage has high stiffness compared with the skin, any amplitude disturbance is observed during the contact between the indenter and the skin. Therefore, the device works in an open loop with a sufficient accuracy.

In order to adapt the device to *in vivo* experimental conditions, the impedance head and the piezoelectric translation stage are placed on an adjustable frame. Indeed, the small force and displacement preclude any manual use. The piezoelectric translation stage is fixed on a high-resolution manual translation stage, associated with a digital micrometer that allows control of the indenter penetration by about 1 μm . This manual translation stage is placed on a rotary plate ring with 4 arc-sec resolution so that the indenter will be perpendicular to the skin whatever the area. A camera makes the positioning of the indenter easier. The whole device is placed on a mobile adjustable frame with a granite base. A schematic diagram of the device is shown in Fig. 2.

Acquisition and generation of signals are carried out by a 16-bit digital-analog I/O card (National Instruments, Austin, TX, USA). A complete software has been developed for this task. This software carries out the acquisition of data and also generates the driving signal performing a frequency scan from 10 to 60 Hz. The sample frequency of the measured signals is 40 kHz and the frequency step of the scan is 5 Hz. As the displacement and force amplitude are very small, a breath or a heart beat can disturb signals. Therefore, to avoid this difficulty, a Fast Fourier Transform is applied to the signals to extract the only component due to the excitation force. The magnitudes f_0 and u_0 and the phasingout φ between both signals are thus obtained. Stiffness and damping are then calculated using Eqs (8) and (9).

Force vs. acceleration is plotted on a Lissajous graph to observe the linearity and damping of the tested materials. Pure elastic materials produce a

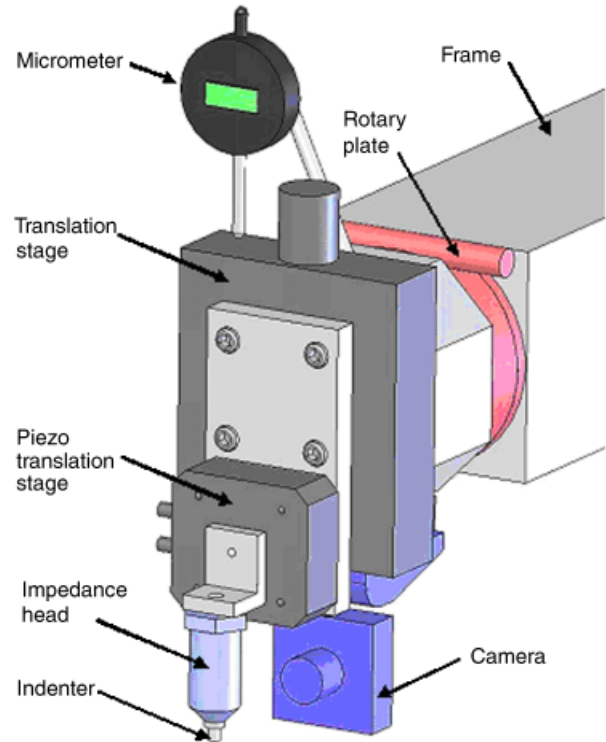


Fig. 2. Diagram of the developed device.

line, whereas viscoelastic materials produce an ellipse (Fig. 3).

Validation on inert material

First, a frequency scan without contact is made to confirm that any parasitic phasingout is introduced by the system. As there is pure inertia on the force sensor, the theoretical phasingout between force and acceleration is 180° . Measurements show a disturbance phasingout of $<0.5^\circ$ (Fig. 4).

The developed device has been tested and validated on helicoidal springs with various stiffnesses. As springs can be considered to be pure elastic material, stiffness should be independent of the frequency stress and the damping should be equal to 0. The phasingout should be equal to 0° before the natural angular frequency and equal to 180° after the natural angular frequency.

Two springs were used, with 80 and 100 N/m stiffnesses (supplier values). Measurements (Fig. 5) and mean values (Table 1) on a frequency scan show the validity of the device. As there is no influence of the experimenter on the device during measurement, inter-experimenter reproducibility on a frequency scan is $<2\%$ for the stiffness.

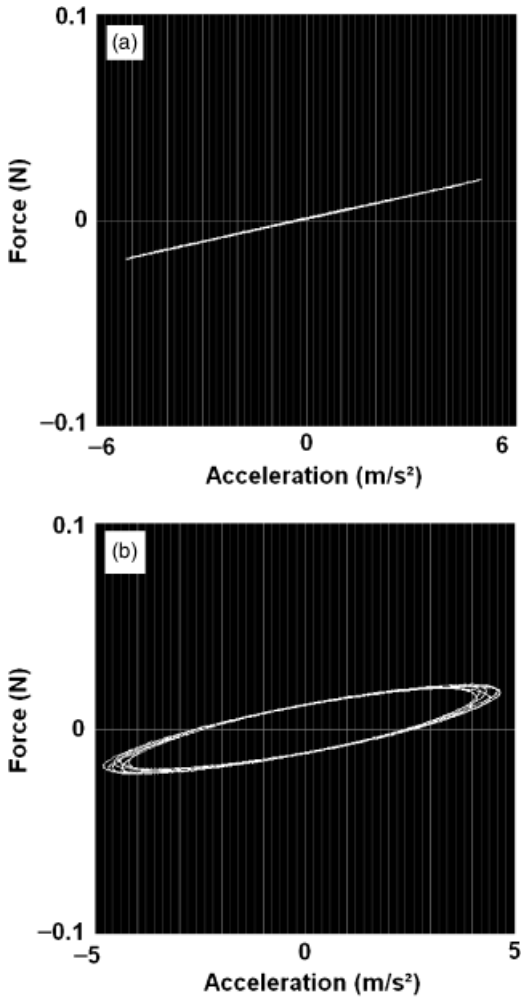


Fig. 3. Example of Lissajous graph for (a) pure elastic and (b) viscoelastic material.

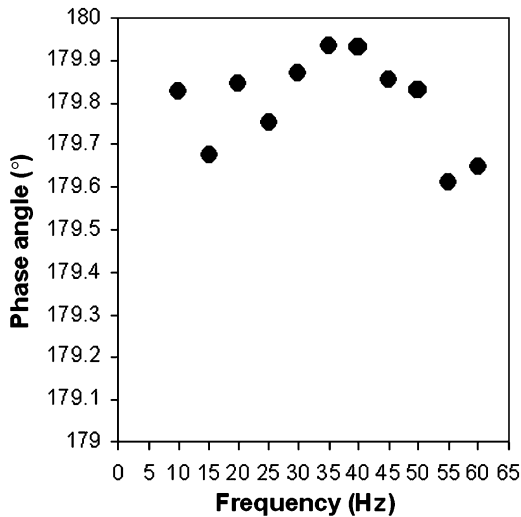


Fig. 4. Phasingout between force and acceleration without contact.

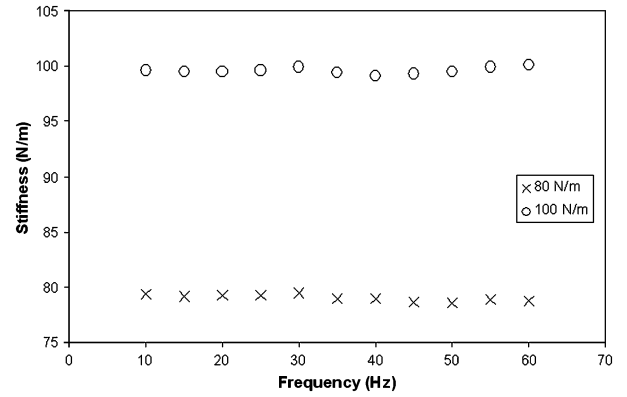


Fig. 5. Stiffness measured on two helicoidal springs.

TABLE 1. Stiffness and damping (mean \pm SD) measured on two helicoidal springs

Spring (N/m)	Stiffness (N/m)	Damping (Ns/m)
80	79 \pm 0.3	<0.01
100	99.6 \pm 0.3	<0.01

SD, standard deviation.

Contact detection

One of the most important steps of the protocol is detecting the contact between the indenter and the skin. Indeed, depending on indenter penetration, the stressed area will be different. This detection is made by measuring the phasingout between force and acceleration signals. Without contact, the impedance head measures pure inertia. The theoretical phasingout is then 180°. As soon as there is contact, the phasingout decreases due to the damping of the skin. As this phasingout follows an arctangent function [Eq. (4)], detection is performed at a low frequency (15 Hz) to maximize the difference with the phasingout without contact. An accuracy of about 1 μ m is obtained with this method.

Other materials

Suction material

The device used for the suction test is the Cutometer[®] MPA 580 (Courage & Khazaka, Köln, Germany) (21). Negative air pressure is applied to the skin surface through the probe aperture. The resulting vertical displacement of the skin into the suction chamber is measured by a non-contact optical system. A spring is placed inside the probe head to apply constant pressure during application to the skin. The probe is fixed to the skin using a double-sided adhesive tape.

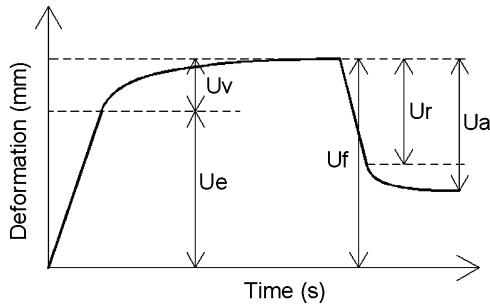


Fig. 6. Skin deformation curve obtained with Cutometer[®].

The time-strain mode is used. A partial vacuum is created over a selected time, followed by a relaxation time. A typical skin deformation curve is illustrated in Fig. 6.

The parameters obtained are :

U_e : Immediate deformation, extensibility

U_v : Viscoelastic contribution, plasticity

U_r : Immediate retraction

U_f : Final deformation, distensibility

U_a : Final retraction after removal of the vacuum

U_r/U_e : Biological elasticity, without viscous deformation

U_r/U_f : Biological elasticity

U_a/U_f : Gross elasticity of the skin, including viscous deformation

U_v/U_e : The ratio of viscoelastic to elastic distension

Hydration measurement

The device used to assess the hydration level is the Corneometer CM 825 (Courage & Khazaka) (22). It is a skin capacitance meter that measures epidermal hydration. This device determines the water content of the superficial epidermal layers down to a depth about 0.1 mm and expresses the values in arbitrary units. A low value corresponds to a dry skin.

Skin replicas

Skin replicas of the inner face of the forearm were made using a silicone rubber (Silflo[®], Flexico developments Ltd, Potters Bar, UK). The skin microrelief in negative replica was studied by confocal microscopy with white light chromatic aberration Altisurf 500[®] (MCE Technologies, Evian les Bains, France). 3×3 mm surface areas were analysed. The means of the area contained between tensing lines of skin, called the plates area, were calculated with Toposurf[®] software (24, 25).

BMI

The BMI is defined by

$$\text{BMI} = \text{weight (kg)}/\text{height (m)}^2 \quad (13)$$

Experimental procedure

Subjects

Measurements *in vivo* have been taken from 46 healthy women volunteers, aged from 18 to 70. They were divided into three age groups (Table 2). All volunteers gave their informed consent, they were free from pathological findings on their arms and had not used any topical agents on the tested area for 72 h.

Protocol

Measurements are made after 30 min of stabilization in a room with controlled temperature and humidity (22 °C and RH 50%). Subjects are seated in a medical chair with a specially designed armrest. The right forearm is fixed by the wrist to minimize movement. Measurements are made 6 cm from the elbow. At first, the indentation test is realized with 200 μm penetration, a displacement amplitude of 3 μm , a frequency ranging from 10 to 60 Hz and an increment of 5 Hz. The total time for a frequency scan is about 40 s. Three scans with complete repositioning of the indenter are made. Secondly, the hydration level is measured. After soft drying the area, three measurements are taken at three close sites. The average of these three measurements is used in subsequent calculations. Thirdly, the suction test is realized, with a pressure of 400 mbar for 3 s, a relaxation period of 5 s and a diameter aperture of 2 mm. Finally, a replica of the studied area is made.

Statistical analysis

Values obtained are expressed as mean \pm standard deviation (SD). The data are analysed by Statgraphic[®] software. For dynamic indentation, the average value from the three frequency scans is used. Analysis of variance (ANOVA) is used to compare age groups. Linear regression is used to

TABLE 2. Subject distribution

Group	Size
1	16 people 18–30 years
2	15 people 31–50 years
3	15 people 51–70 years

study relations between measurement and age, and between all the parameters. A value of P smaller than 0.05 is considered to be statistically significant.

Results

As the skin thickness is not measured, only the contact parameters of dynamic indentation (K and C) and the parameters of the suction test, which are independent of skin thickness (U_r/U_f and U_v/U_e), are compared (7). U_r/U_e is not reported because it paralleled U_r/U_f .

In vivo behaviour of human skin under dynamic indentation

Measurements *in vivo* show that stiffness, damping and phasingout between force and acceleration can be described by a Kelvin–Voight model: a purely viscous damper and a purely elastic spring whose physical characteristics are independent of the stress frequency (Figs 7–9). The average SD on each frequency scan is <5% of the

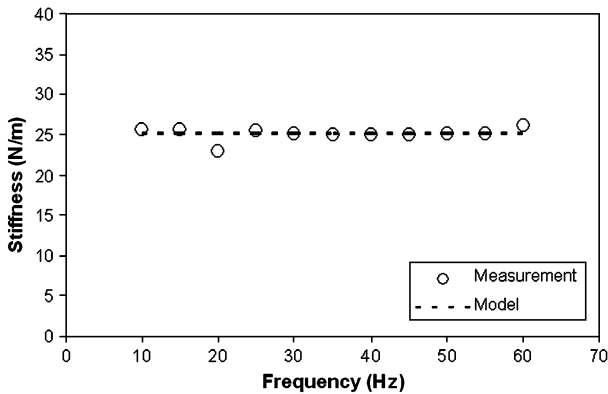


Fig. 7. Comparison between measured stiffness and Kelvin–Voight model ($K(\omega) = \text{constant}$).

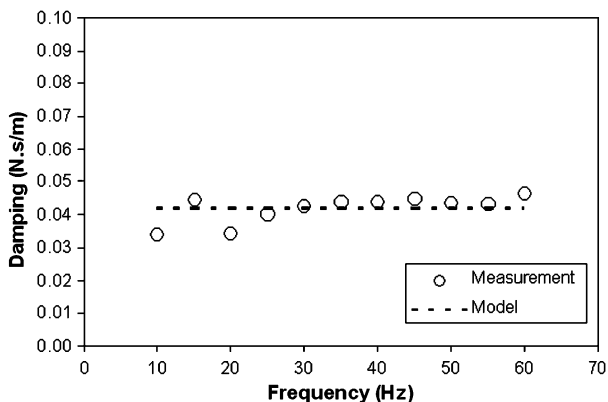


Fig. 8. Comparison between measured damping and Kelvin–Voight model ($C(\omega) = \text{constant}$).

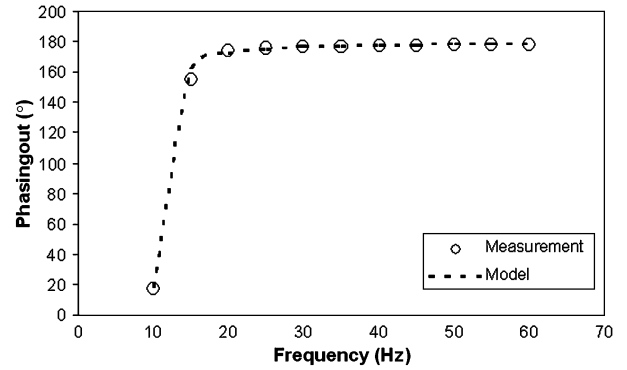


Fig. 9. Comparison between experimental phasingout and Kelvin–Voight model.

average value for the stiffness, and <15% of the average value for the damping.

At each frequency, the standard error for three successive *in vivo* measurements is between 4% and 7% of the mean value. A reference spring was measured every five subjects. The stiffness variability throughout the study is <1.5%. This shows the good reproducibility of the device.

The average values of stiffness and damping on a frequency scan are used to compare different subjects. The values for each group are given in Table 3.

The complex modulus [Eqs (10)–(12)] has a real part that is independent of the stress frequency, and an imaginary part that is dependent on the stress frequency. The values of these parameters for 10 Hz stress frequency are given in Table 4.

Correlation between dynamic indentation, suction test and topographic parameters

Elasticity and stiffness

The ANOVA study shows a statistically significant difference between age groups for stiffness K (Fig. 10, $P = 0.0002$) and biological elasticity U_r/U_f (Fig. 11, $P = 0.0027$). Both parameters decrease with age. Moreover, a correlation coefficient up to 0.5 for both parameters ($r = 0.6$ for K and $r = 0.54$ for U_r/U_f) is observed (Figs 12 and 13). Suction test values for each group are shown in Table 3. There is a weak correlation coefficient between biological elasticity and stiffness (Fig. 14, $r = 0.35$).

Viscosity and damping

The ANOVA study shows no statistical differences between age groups for damping C (Fig. 15, $P = 0.0847$) and for the ratio between delayed

TABLE 3. Mean \pm SD for dynamic indentation, suction test and replica parameters

Group	K (N/m)	C (Ns/m)	U_r/U_f	U_v/U_e	Area (mm ²)
1	42.5 \pm 10.6	0.074 \pm 0.019	0.687 \pm 0.105	0.308 \pm 0.071	0.072 \pm 0.008
2	32.1 \pm 7.4	0.063 \pm 0.014	0.605 \pm 0.115	0.357 \pm 0.063	0.087 \pm 0.019
3	28.4 \pm 8.2	0.062 \pm 0.016	0.532 \pm 0.131	0.355 \pm 0.069	0.113 \pm 0.038

SD, standard deviation.

TABLE 4. Real, imaginary and complex modulus of each group at 10 Hz

Group	E'^* (kPa)	E''^* (kPa)	E^* (kPa)
1	10.6 \pm 2.6	1.17 \pm 0.31	10.7 \pm 2.64
2	8 \pm 1.8	0.99 \pm 0.21	8.09 \pm 1.84
3	7.1 \pm 2.1	0.98 \pm 0.25	7.17 \pm 2.06

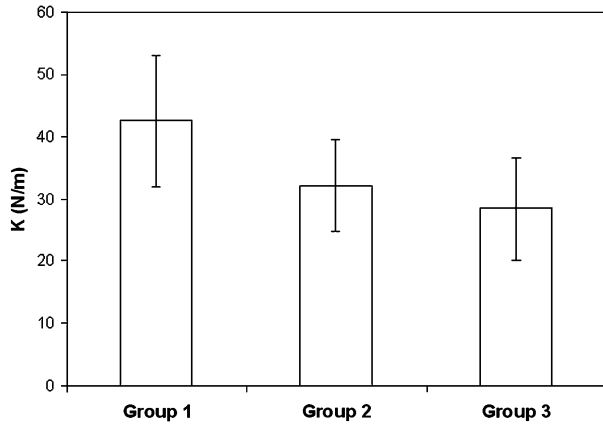


Fig. 10. Stiffness K for each age group ($P = 0.0002$).

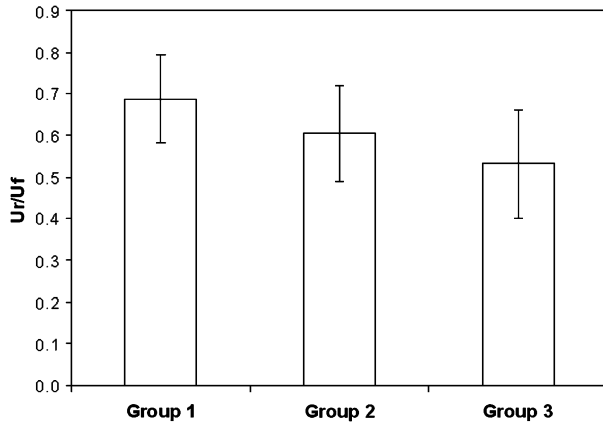


Fig. 11. Biological elasticity U_r/U_f for each age group ($P = 0.0027$).

and immediate deformation U_v/U_e (Fig. 16, $P = 0.0841$). U_v/U_e increases between groups 1 and 2 and is constant between groups 2 and 3, and damping C declines between groups 1 and 2 and is constant between groups 2 and 3. A correlation coefficient with age of 0.35 is found for both parameters. Damping C and U_v/U_e are not correlated ($P > 0.05$). The values of the ANOVA

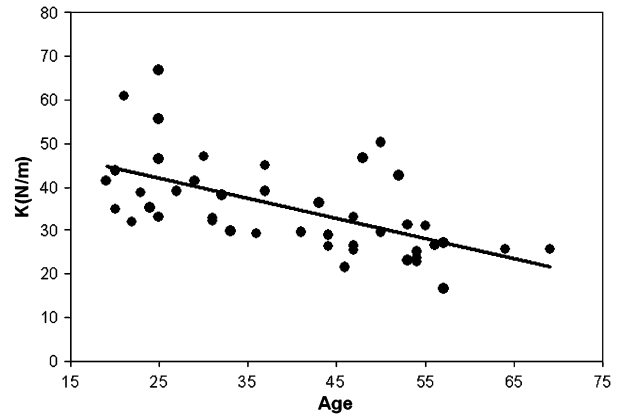


Fig. 12. Linear regression between stiffness and age ($r = 0.6$).

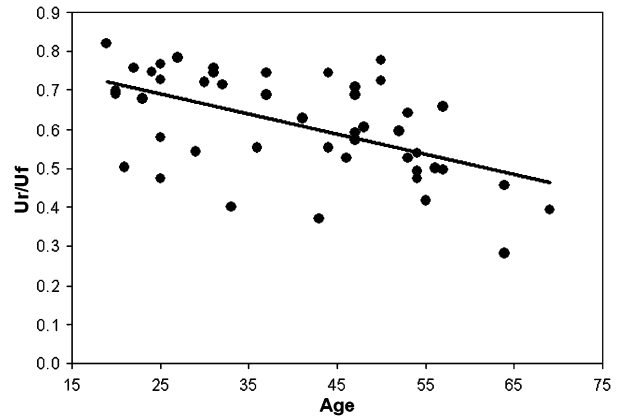


Fig. 13. Linear regression between biological elasticity and age ($r = 0.54$).

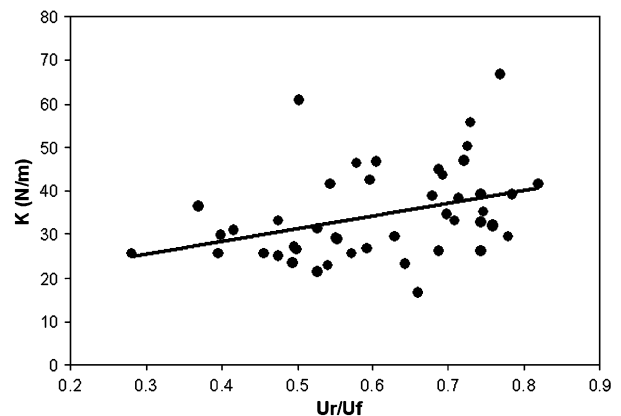


Fig. 14. Linear regression between biological elasticity and stiffness ($r = 0.35$).

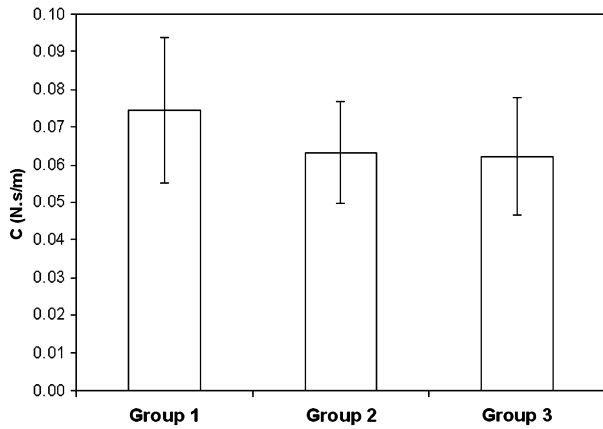


Fig. 15. Damping C for each age group ($P = 0.0847$).

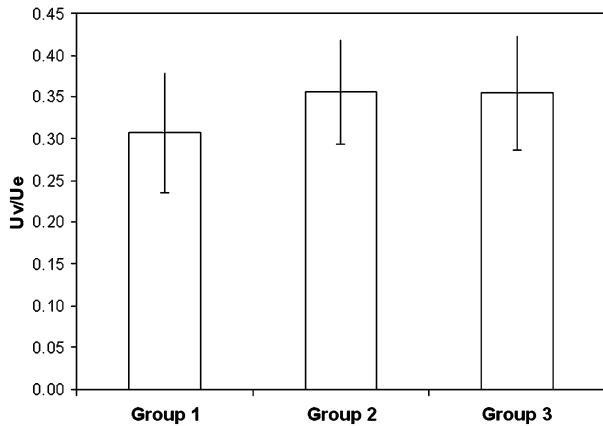


Fig. 16. U_v/U_e for each age group ($P = 0.0841$).

study and linear regression for all parameters are shown in Tables 5–7.

Plates area

The ANOVA study shows a statistically significant difference between age groups for plates area (Fig. 17, $P = 0.0002$). Area increases with age. Figure 18 shows topographic representations and plates area representative pictures of the skin for each group. A good linear regression between plates area and age is shown, with an increase of this parameter with age (Fig. 19, $P = 0.58$). There is a good correlation coefficient between stiffness K and area (Fig. 20, $r = 0.54$), and between damping C and area (Fig. 21, $r = 0.43$). However, suction parameters and plates area are not correlated ($P > 0.05$).

Hydration level

The ANOVA study shows a statistically significant difference between age groups for the hydration level (Fig. 22, $P = 0.0014$). The hydration level

TABLE 5. ANOVA values for comparison between each group

Parameter	P ANOVA
K	0.0002
C	0.0847
U_r/U_t	0.0027
U_v/U_e	0.0841
Area	0.0002
Hydration level	0.0014
BMI	0.6846

SD, standard deviation; BMI, body mass index; ANOVA, analysis of variance.

TABLE 6. Linear regression of each parameter with age: P value and correlation coefficient r

Parameter	P	r
K	<0.0001	0.6
C	0.018	0.35
U_r/U_t	0.0001	0.54
U_v/U_e	0.0171	0.35
Area	<0.0001	0.58
Hydration level	<0.0001	0.59
BMI	0.53	0.09

BMI, body mass index.

TABLE 7. Linear regression between parameter: P value and correlation coefficient r

Parameters	P	r
K and U_r/U_t	0.0156	0.35
C and U_v/U_e	0.7527	0.048
K and area	0.0001	0.54
C and area	0.028	0.43
U_r/U_t and area	0.0813	0.26
U_v/U_e and area	0.7307	0.052

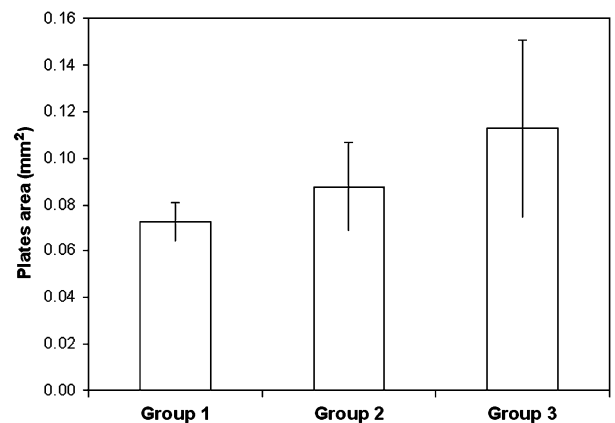


Fig. 17. Plates area for each group ($P = 0.0002$).

increases with age. The biological elasticity U_r/U_t is better correlated with the hydration level than the stiffness and the damping (Figs 23–25). There is no correlation between U_v/U_e and plates area

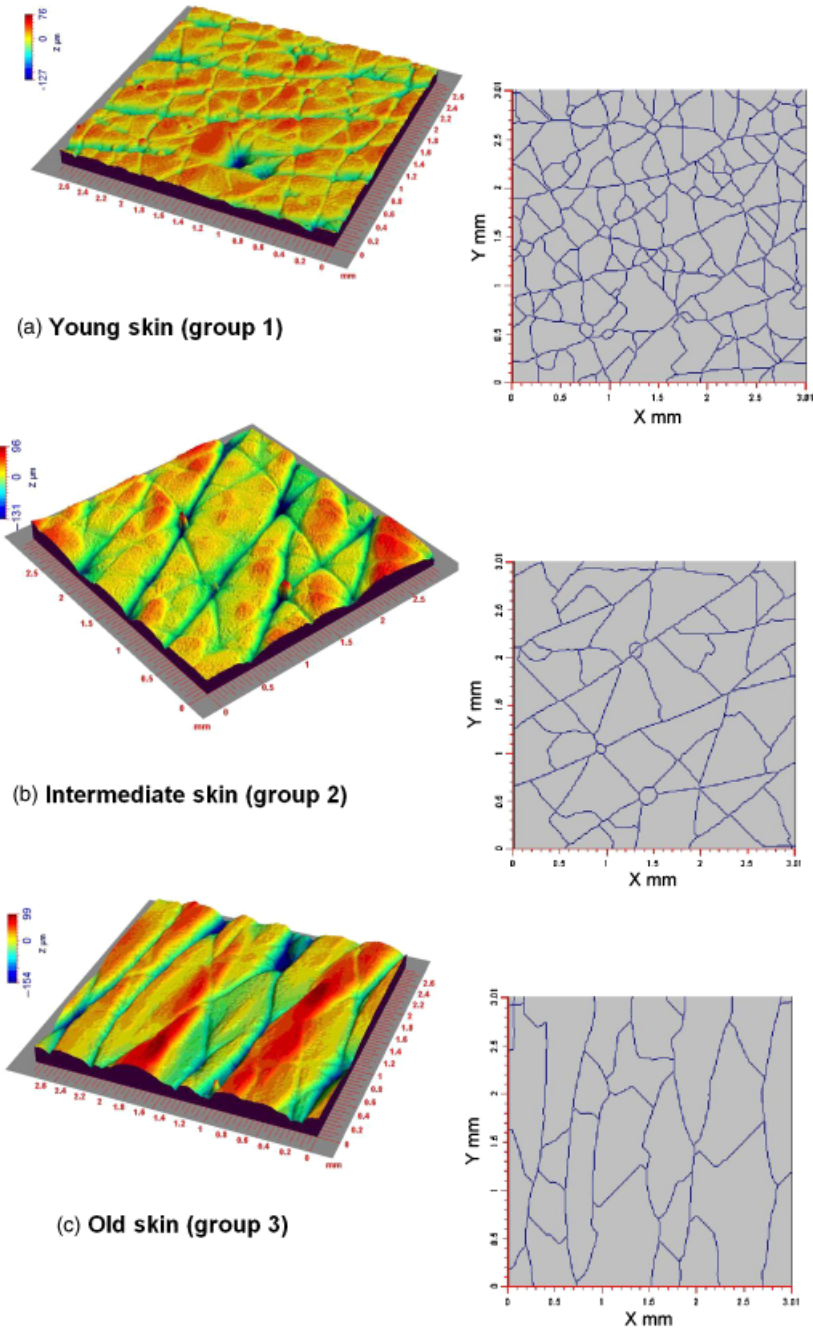


Fig. 18. Topographic representation and representative picture of plates area: (a) young skin (b) intermediate skin and (c) old skin.

with hydration ($P > 0.05$). The values of the linear regression for the hydration level are shown in Table 8.

BMI

ANOVA study shows no statistical difference between age groups for the BMI ($P = 0.6846$). There is no correlation of the BMI with other parameters ($P > 0.05$), except for the damping C ($P = 0.0349$, $r = 0.31$). Damping increases with

the BMI (Fig. 26). The values of the linear regression for the BMI are shown in Table 9.

Discussion

Dynamic mechanical analysis using indentation is often used on polymer materials, and the principle has been known for a long time. However, its application on human skin *in vivo* is unusual. In this paper, a complete developed device with an amplitude strain from 1 to 10 μm

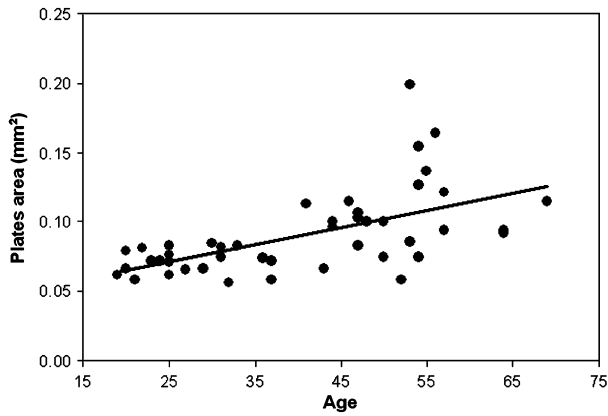


Fig. 19. Linear regression between plates area and age ($r = 0.58$).

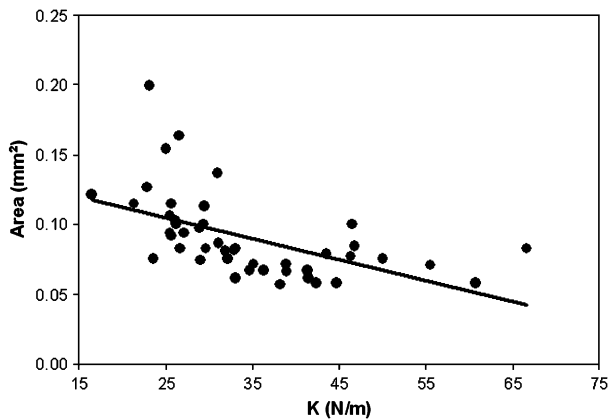


Fig. 20. Linear regression between plates area and stiffness ($r = 0.54$).

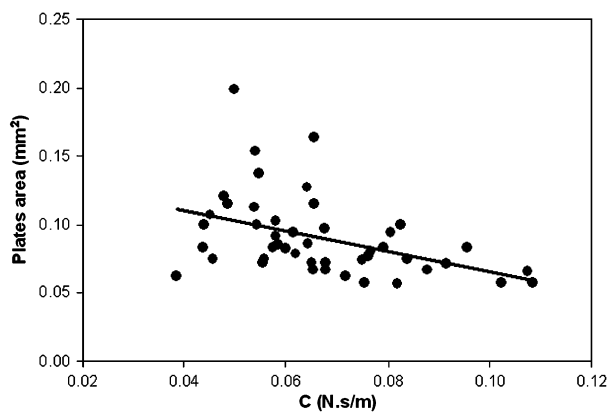


Fig. 21. Linear regression between plates area and damping ($r = 0.43$).

and a frequency ranging from 10 to 60Hz has been presented. Tests on pure elastic inert materials have proved its validity and its reproductibility for stiffness and damping measurement.

The results obtained with the Cutometer[®] agree with other studies (5). The biological elasticity ratio U_r/U_f decreases with age, and U_v/U_e

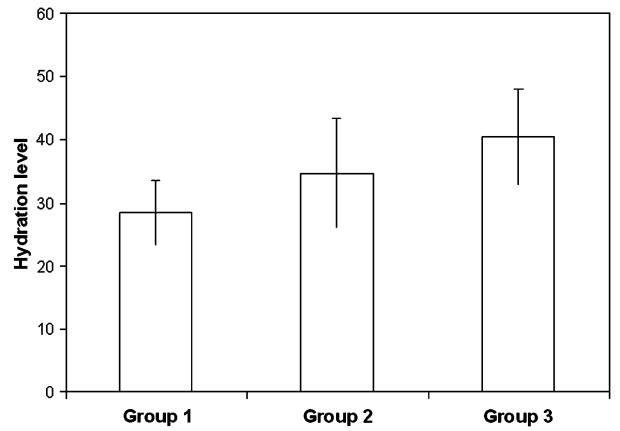


Fig. 22. Hydration level for each group ($P = 0.0014$).

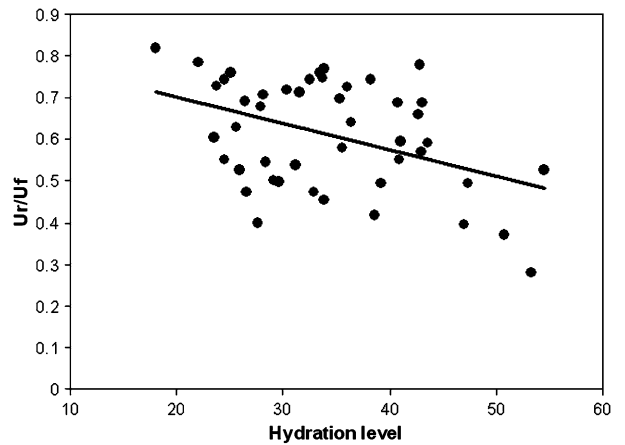


Fig. 23. Linear regression between biological elasticity and hydration level ($r = 0.42$).

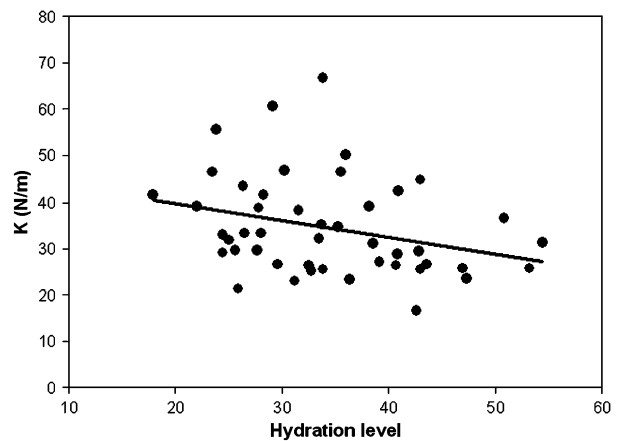


Fig. 24. Linear regression between stiffness and hydration level ($r = 0.3$).

increases. These parameters show that the skin become less elastic and more viscous with age.

Dynamic indentation results with a $3\mu\text{m}$ displacement amplitude on each subject show that a

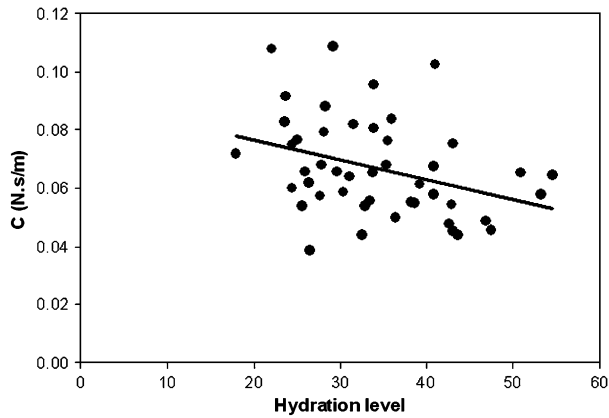


Fig.25. Linear regression between damping and hydration level ($r = 0.35$).

TABLE 8. Correlation between hydration level and other parameters

Parameter	P	r
K	0.04	0.3
C	0.018	0.35
U_r/U_t	0.0039	0.42
U_v/U_e	0.1836	0.2
Area	0.49	0.104

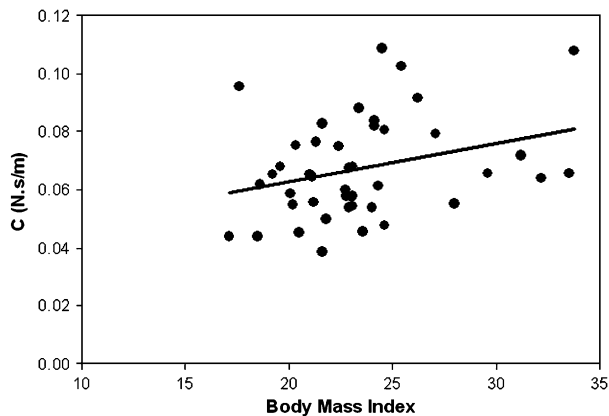


Fig.26. Linear regression between damping and body mass index ($r = 0.31$).

Kelvin–Voight model can be used to describe the mechanical behaviour of the skin with a frequency stress ranging from 10 to 60 Hz. The average of stiffness and damping is sufficient to compare different measurements. The good reproducibility on human skin *in vivo* has been proved. The results show that the indenter-skin contact stiffness and damping decrease with age.

As a whole, a decline of the complex modulus with age is found. This result disagrees with other Cutometer[®] studies, which found an increase of Young modulus with age (26–28).

This difference can be explained by the fact that dynamic indentation measurements were

TABLE 9. Correlation between body mass index and other parameters

Parameter	P	r
K	0.388	0.13
C	0.0349	0.31
U_v/U_e	0.7283	0.05
U_r/U_t	0.81	0.036
Area	0.556	0.089

performed without a guard ring. Contrary to the suction test, no skin area is marked off. Dynamic indentation measures the natural state of tension of the skin, and the Cutometer[®] measures its intrinsic rheological properties. This phenomenon is similar to the measurements made by torsion with or without a guard ring (29). The results found are also coherent, because the skin is less tense (lowering of the complex modulus measured by dynamic indentation) and stiffer (increase of the modulus measured by a suction test) with age (26).

Moreover, as the natural tensing of the skin is due to the collagen and elastin network of the dermis, the good correlation between the plates area (which corresponds to this network) with stiffness and damping confirms that dynamic indentation concerns mainly the natural tense state of the skin. Suction test parameters are less correlated with the plates area because the 2-mm-diameter aperture suction chamber used concerns mainly the epidermis properties (5).

The results show that the hydration level has a slight influence on the stiffness, the damping and the biological elasticity. As the hydration level measured corresponds to the epidermis, this layer seems to have a slight influence on the measurement.

The correlation between the BMI and the damping shows that the hypodermis may influence this parameter slightly. However, no correlation with other parameters has been found.

The complex modulus found is similar to results with static indentation from the literature. Jachowicz et al. (3) found a Hertz modulus on 28–65-year-old women's forearms in the range of 7–22 kPa with an indentation force of 0.06 N. Paillet-Mattei and Zahouani (30) found a reduced Young's modulus on 30-years-old women's forearms of 9.5 ± 2 kPa with a penetration of 2000 μm . The advantage of dynamic indentation is that it takes into account the stress velocity with only one frequency scan.

The weak correlation between dynamic indentation and the Cutometer[®] is not surprising, because the devices are based on different principles. However, the results found with both devices in this study are consistent.

In conclusion, dynamic indentation seems to be a good method to access the natural tense state of the skin on the body with a stiffness and damping measurement. The small stress amplitude and indenter penetration minimizes the effects of underlying structures, although the correlation of the damping with the BMI shows that the hypodermis, the deepest layer, influences this parameter. The device presented has some advantages: a small contact area, absence of an adhesive, possibility of performing *in vitro* and *in vivo* studies, good reproductibility and possibility of realizing several successive measurements without changing the skin properties. Moreover, the fact that the experimenters do not hold the device during measurement gives excellent inter-experimenter reproducibility. However, the high sensibility requires strict experimental conditions for *in vivo* application. Measurements of stiffness and damping with this device are complementary to viscoelastic phenomenological parameters of the suction test.

Acknowledgement

The authors wish to thank Peritesco laboratory (Paris, France) for supporting this study.

References

1. Agache P, Humbert P. Measuring the skin. New York: Springer-Verlag, 2004.
2. Zahouani H, Pailler Mattei C, Vargiolu R, Abellan MA. Assessment of the elasticity and tactile properties of the human skin surface by tribological tests. 22nd IFSCC Congress, Edinburgh, 2002.
3. Jachowicz J, McMullen R, Prettypaul D. Indentometric analysis of *in vivo* skin and comparison with artificial models. *Skin Res Technol* 2007; 13: 299–309.
4. Dellaleau A, Josse G, Lagarde JM, Zahouani H, Berghéau JM. Characterization of the mechanical properties of skin by inverse analysis combined with the indentation test. *J Biomech* 2006; 39: 1603–1610.
5. O'goshi K. Suction chamber method for measurement of skin mechanics: the Cutometer[®]. Handbook of non-invasive methods and the skin, 2nd edn. CRC Press, USA: New York; 2006: 579–582.
6. Diridollou S, Patat F, Gens F et al. *In vivo* model of the mechanical properties of the human skin under suction. *Skin Res and Technol* 2000; 6: 214–221.
7. De Rigal J. Hardware and basic principles of the Dermal Torque Meter. Bioengineering of the skin–skin biomechanics. CRC Press, USA: New York; 2002: 63–76.
8. Agache PC, Monneur C, Lévêque JL, De Rigal J. Mechanical properties and Young's modulus of human skin *in vivo*. *Arch Dermatol Res* 1980; 269: 221–232.
9. Genissou JL. Le palpeur acoustique: un nouvel outil d'investigation des tissus biologiques. Ph.D. thesis, Université Paris 6, France, 2003.
10. Vescovo P, Varchon D, Humbert P. *In vivo* tensile tests on human skin: the extensometers. Bioengineering of the skin–skin biomechanics. CRC Press, USA: New York; 2002: 77–90.
11. Tacker JG, Lachetta FA, Allaire PE, Edgerton MT, Rodeheaver GT, Edlich RF. *In vivo* extensometer for measurement of the biomechanical properties of human skin. 1977; 48: 181–185.
12. Pugliese PT, Potts JR. Hardware and basic principles: the Ballistometer. Bioengineering of the skin–skin biomechanics. CRC Press, USA: New York; 2002: 147–160.
13. Barbenel JC, Evans JH. The time-dependent mechanical properties of skin. *J Invest Dermatol* 1977; 69: 318–320.
14. Christensen MS, Hargens CW, Nacht S, Ganz EH. Viscoelastic properties of intact human skin: instrumentation, hydration effects, and the contribution of the stratum corneum. *J Invest Dermatol* 1977; 69: 282–286.
15. Menard KP. Dynamic mechanical analysis: a practical introduction, 1999. Boca Raton, FL: CRC Press.
16. Vriend NM, Kren AP. Determination of the viscoelastic properties of elastometric materials by the dynamic indentation method. *Polym Test* 2004; 23: 369–375.
17. Yin Y, Ling S, Liu Y. A dynamic indentation method for characterizing soft incompressible viscoelastic material. *Mater Sci Eng* 2004; 379: 334–340.
18. Odegard GM, Gatesa TS, Herring HM. Characterization of viscoelastic properties of polymeric materials through nanoindentation. *Exp Mech* 2005; 45: 130–136.
19. Johnson KL. Contact Mechanics. Cambridge: Cambridge University Press.
20. Pailler Mattei C, Zahouani H. Study of adhesion forces and mechanical properties of human skin *in vivo*. *J Adhes Sci Technol* 2004; 18: 1739–1758.
21. Barrel AO, Courage W, Clarys P. Suction chamber method for measurement of skin mechanics: the new digital version of the cutometer[®]. Handbook of non-invasive methods and the skin, 2nd edn. CRC Press, USA: New York; 2006: 583–592.
22. Gabard B, Clarys P, Barrel AO. Comparison of commercial electrical measurement instruments for assessing the hydration state of stratum corneum. Handbook of non-invasive methods and the skin, 2nd edn. CRC Press, USA: New York; 2006: 351–358.
23. Mignot J. Three-dimensional evaluation of skin surface: Micro- and Macrorelief. Handbook of non-invasive methods and the skin, 2nd edn. CRC Press, USA: New York; 2006: 179–193.
24. Zahouani H. Indentification de la signature morphologique du vieillissement de la surface cutanée par les lignes de partage des eaux et la décomposition en ondelettes continues. Actualités en ingénierie cutanée, Vol. 4.
25. Zahouani H, Lefur I, Vargiolu R, Morizot F, Lambrosine L, Guinot C, Tschachler E. Determination of ageing speed and the index of elasticity loss of Caucasian and Japanese women. World Congress on Noninvasive Studies of the skin. *Skin Res Technol* 2005; 11: 291–299.
26. Diridollou S, Vabret V, Berson M, Vaillant L, Black D, Lagarde JM, Grégoiret JM, Gall Y, Patat F. Skin ageing: changes of physical properties of human skin *in vivo*. *Int J Cosmet Sci* 2001; 23: 353–362.

27. Grahame R, Holt PJ. The influence of ageing on the in vivo elasticity of human skin. *Gerontologica* 1969; 15: 121–139.
28. Alexander H, Cook T. Variations with age in the mechanical properties of human skin. *J Tissue Viability* 2006; 16: 6–11.
29. de Rigal J, Lévêque JL. Influence of aging on the mechanical properties of skin. In Lévêque JL and Agache PG, Eds. *Aging skin-properties and functional changes*, 1993. Informa Healthcare, UK: London. p. 15–28.
30. Pailler-Mattei C, Zahouani H. Analysis of adhesive behaviour of human skin in vivo by an indentation test. *Tribol Int* 2006; 39: 12–21.

Address:

Gaëtan Boyer

Laboratory of Tribology and System Dynamics

UMR CNRS 5513

ENISE-ECL

36 Avenue Guy de Collongue

69131 Ecully

France

Tel: +33 6 8506 6915

Fax: +33 4 7843 3383

e-mail: gaetan.boyer@ec-lyon.fr